Multiphase Structure of Segmented Polyurethanes: Effects of Hard-Segment Flexibility

Yingjie Li,† Zhiyong Ren,‡ Ming Zhao,‡ Huichang Yang,‡ and Benjamin Chu*,†,§

Department of Chemistry, State University of New York at Stony Brook, Long Island, New York 11794-3400, Henan Institute of Chemistry, Zhengzhou, People's Republic of China, and Department of Materials Science and Engineering, State University of New York at Stony Brook, Long Island, New York 11794

Received June 4, 1992; Revised Manuscript Received October 16, 1992

ABSTRACT: Synchrotron small-angle X-ray scattering (SAXS) and differential scanning calorimetry (DSC) were used to investigate the structure of a few series of segmented polyurethanes with different hard-segment flexibilities. The segmented polyurethanes based on 1,6-hexamethylene diisocyanate (HDI) and 1,4-butanediol (BD) as the hard segment showed a folded-chain conformation. The phase structure was found to be insensitive to the increasing hard-segment content and thermal treatment. Phase separation was very fast in these systems as the hard-segment mobility was relatively high and the system viscosity was low. DSC results showed a soft-segment glass transition temperature which was only about 5 °C above that of the pure soft segment, indicating that the separation between soft and hard segments was nearly complete. The segmented polyurethanes based on 4,4'-methylenebis(phenyl isocyanate) (MDI) and 4,4'-diaminodiphenyl ether (DDE) probably did not exist in the folded-chain conformation. DSC results showed a soft-segment glass transition temperature which was about 15 °C above that of the pure soft segment. Both systems showed very strong interactions among the hard segments. Results were discussed based on the viscosity–mobility–interaction argument. In addition, a long-time controversy about the dependence of $T_{g,s}$ upon the chemical structure of the soft and hard segments and the soft- and hard-segment lengths could be explained by the viscosity–mobility–interaction argument. The present study once again suggested the importance of kinetic effects in formulating a better understanding of the structure–property relationships of segmented polyurethanes.

I. Introduction

Thermoplastic segmented polyurethane elastomers are linear $-[A-B]_n-$ block copolymers. One of the blocks is relatively flexibile with a low solubility parameter and is referred to as the soft segment while the other block is either highly polar and/or stiff with a high solubility parameter and is known as the hard segment. The incorporation of them gives rise to a material with novel and unique characteristics. It is generally accepted that the good properties of this class of materials are owing to the microphase-separated structure. The structure–property relationship has been a topic of intense academic and industrial research.[1]

Early studies mainly concentrated on those segmented polyurethanes based on 4,4'-methylenebis(phenyl isocyanate) (MDI) or toluene diisocyanate (TDI) with 1,4-butanediol (BD) as the chain extender.[1] By using wide-angle X-ray diffraction (WAXD) and small-angle X-ray scattering (SAXS), Bonart et al.[2] proposed a model that the hard segments existed as extended chains. Recently, on the basis of results from SAXS and thermal analysis, Koberstein and Stein[3] and later Leung and Koberstein[4] proposed a model that the thickness of the hard-segment domains was controlled by the shortest hard-segment chain insoluble in the soft-segment phase. Hard segments longer than this critical length were either coiled or even folded in order to be in the hard-segment domain. Hard segments shorter than this critical length were dissolved in the soft-segment phase. In earlier studies,[5-8] we observed that the system viscosity, the hard-segment mobility, and the strength of the hard-segment interaction among themselves depended upon the annealing temperature and were important factors governing the structure of segmented polyurethanes. In MDI/BD-based segmented polyurethanes, the system viscosity was high, the hard-segment mobility was low, and the interactions among the hard segments were strong. These characteristics resulted in very slow phase separation after the melt was quenched to lower annealing temperatures. The phase separation process could be described by an equation of relaxation. The postannealing of a sample in equilibrium had little effect once the interactions among the hard segments reached a certain strength. Above 120 °C, spherulites could be observed.

The viscosity–mobility–interaction argument basically emphasized the *kinetic* effects. It could be tested by intentionally changing the flexibility of the hard segment. Aliphatic diisocyanates like 1,6-hexamethylene diisocyanate (HDI) with BD as the chain extender give hard segments with greater flexibility when compared with MDI/BD. According to the argument, the phase separation rate should be increased owing to the relatively higher hard-segment mobility and lower system viscosity. If the kinetic effect is the controlling factor, the phase separation should have a better chance to reach equilibrium due to the higher hard-segment mobility. If the thermodynamic effect is the controlling factor, the phase separation process could be less complete when compared with the MDI/BD system, because of the relatively lower thermodynamic incompatibility between the hard and soft segments in the HDI/BD system (Table I). On the other hand, if the aliphatic BD in MDI/BD is replaced by an aromatic diamine, the thermodynamic incompatibility between the hard and soft segments is increased due to the introduction of urea groups (Table I). The interaction between the hard segments should also be stronger due to the three-dimensional hydrogen-bonding ability, which

* To whom all correspondence should be addressed (use Chemistry address).
† Department of Chemistry, State University of New York at Stony Brook.
‡ Henan Institute of Chemistry.
§ Department of Materials Science and Engineering, State University of New York at Stony Brook.

0024-9297/93/2226-0612$04.00/0

Table I
Estimated Solubility Parameters for the Segmented Polyurethanes[a]

segment	solubility parameter
PTMO	8.7
PES	10.2
HDI/BD	10.7[b]
MDI/BD	11.5
MDI/DDE	11.9

[a] Densities were calculated by following van Krevelen (*Properties of Polymers*; Elsevier: New York, 1976). The molar attraction constants were from Hoy (Hoy, K. L. *J. Paint Technol.* **1970**, *42*, 76). Some of the density values could be found from the literature. We could not get the values for all the segments, and the published values are different from different authors. Therefore, all the density values were calculated to get a consistent set of values. The absolute solubility parameters may contain substantial errors. However, the relative tendency should be reasonable. [b] Density was calculated from a crystallinity of 44.4%, based on our DSC values and ref 29.

could be an additional driving force for more complete phase separation.

Industrially, efforts have been made to develop segmented polyurethanes based on aliphatic diisocyanates,[9-15] which exhibit better light stability and better resistance to hydrolysis and thermal degradation. Diamines, although excellent chain extenders, cannot be used for thermoplastic segmented polyurethane elastomers, because the urea groups melt well above the decomposition temperature. However, sterically hindered aromatic diamines in combination with aromatic diisocyanates can result in materials suitable for energy-absorbing applications. This class of materials has also drawn considerable attention.[16-23]

In previous reports,[5,6,14] we have shown different crystallization and spherulite formation behavior of HDI/BD-based samples and MDI/BD-based samples. Both the crystallization process and spherulite formation are fast in HDI/BD-based systems (on the order of minutes) and slow in the MDI/BD-based system (on the order of hours). Upon melt quenching, MDI/BD-based samples formed spherulites after annealing at above 120 °C while HDI/BD-based samples can form spherulites after annealing at or above room temperature. In this paper, we report the synchrotron SAXS and differential scanning calorimetry (DSC) results based on the segmented polyurethanes with different hard-segment flexibilities and different soft- and hard-segment lengths.

II. Experimental Section

Materials. (1) PES/HDI/BD Series. The soft segment is poly(ethylene/propylene adipate) with a molar ratio of ethylene glycol/propylene glycol = 10/1 and $M_n \simeq 2000$ (PES). The hard segment consists of HDI and BD. The samples were prepared by a one-step bulk polymerization and are denoted PES/HDI/BD-xx, where xx represents the hard-segment content (%). The samples used without further treatment are known as the as-reacted samples.

(2) PES/MDI/DDE Series. The soft segment is PES, the same as in the PES/HDI/BD series. The hard segment consists of MDI and 4,4'-diaminodiphenyl ether (DDE). The samples were prepared by a solution polymerization and are denoted PES/MDI/DDE-xx, where xx represents the hard-segment content (%). The PES/MDI/DDE samples could not be melted without decomposition. Only solution-cast samples were used with a dimethyl sulfone/methyl isobutyl ketone (volume ratio = 1:1) mixture as the casting solvent.

(3) PTMO/MDI/DDE Series. The soft segment is poly(tetramethylene oxide) (PTMO) with $M_n \simeq 1000$. The hard segment is MDI/DDE. The samples were prepared by a solution polymerization and are denoted PTMO/MDI/DDE-xx, where xx represents the hard-segment content (%). The PTMO/MDI/DDE samples could not be melted without decomposition. Only solution-cast samples were used with a dimethyl sulfone/methyl isobutyl ketone (volume ratio = 1:1) mixture as the casting solvent.

(4) PES/MDI/BD Series. The soft segment is PES. The hard segment consists of MDI and BD. The samples were prepared by a solution polymerization and are denoted PES/MDI/BD-xx, where xx represents the hard-segment content (%). Only solution-cast samples were used with a dimethyl sulfone/methyl isobutyl ketone (volume ratio = 1:1) mixture as the casting solvent.

(5) PPO–PTMO/MDI/BD Series. The soft segment is poly(tetramethylene oxide) (PTMO) end-capped with poly(propylene oxide) (PPO) with wt % PTMO:PPO = 70:30 (PPO–PTMO). The soft segment has a number-average molecular weight M_n of ~1000 (PPO–PTMO-1000) and ~2000 (PPO–PTMO-2000). The hard segment is MDI/BD. A two-step bulk polymerization was employed, and as-reacted samples were used in the DSC measurements.

All the annealing experiments were performed in vacuum.

Instrumentation. Synchrotron SAXS experiments were performed at the SUNY X3A2 Beamline, National Synchrotron Light Source (NSLS), Brookhaven National Laboratory (BNL). Details about the setup can be found elsewhere.[24,25] A modified Kratky collimation system was used along with a Braun linear position sensitive detector. The X-ray wavelength was 0.154 nm. The adaptation of a special tantalum beam stop with a sharp edge greatly facilitated the SAXS alignment due to improved parasitic scattering background. Smearing effects on the SAXS patterns were negligible. Time-dependent experiments were performed by using a double-cell high-temperature jumper. Routine correction procedures, except the absolute intensity calibration, were performed on the SAXS data.

The SAXS experiments were performed at room temperature, except for the kinetic experiments. We[8] could show that the difference in performing the SAXS experiments of annealed samples at room temperature and of samples at annealing temperature could be taken into account by the thermal expansion effects, provided that the phase separation and crystallization processes were *complete*. Secondary phase separation and crystallization were not significant.

DSC measurements were carried out by using a Perkin-Elmer Model DSC-2C instrument operated at a 20 °C/min heating rate. A sample weight of about 10 mg was used for DSC experiments.

III. Results and Discussion

(1) SAXS Results. For a system with spherical symmetry, the X-ray scattered intensity is related to the so-called normalized three-dimensional correlation function by[26]

$$\gamma_3(r) = (1/Q)\int_0^\infty q^2 I(q)[\sin(qr)/(qr)]\,dq \qquad (1)$$

where $\gamma_3(r) = \langle \eta(\mathbf{r}_1)\eta(\mathbf{r}_2)\rangle/\langle \eta^2\rangle$, $r = |\mathbf{r}_1 - \mathbf{r}_2|$, $\eta(\mathbf{r}_i)$ is the local electron density fluctuation at position $\mathbf{r}_i$, and $\langle \eta^2\rangle$ is the mean square electron density fluctuation. The magnitude of the scattering vector $q = (4\pi/\lambda)\sin(\theta/2)$, with λ and θ being, respectively, the X-ray wavelength and the scattering angle; the invariant Q is defined by the equation

$$Q = \int_0^\infty q^2 I(q)\,dq \qquad (2)$$

For an ideal two-phase system with sharp interfaces

$$Q_{id} \sim \phi_1\phi_2(\rho_1 - \rho_2)^2 \qquad (3)$$

where ϕ_i and ρ_i are the volume fraction and the electron density of the ith phase, respectively. The physical importance of Q is that it is directly related to the mean square fluctuation of the electron density. Thus, Q/Q_{id} can be used as an approximate indication of the overall degree of phase separation.[11] The Q_{id} value of the samples with different thermal treatment remains the same if the same starting sample is used and the measurements are

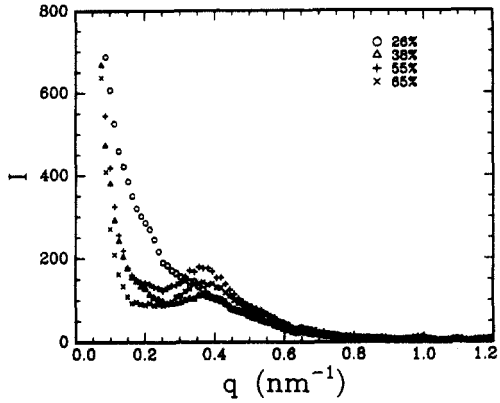

Figure 1. SAXS patterns of as-reacted PES/HDI/BD samples.

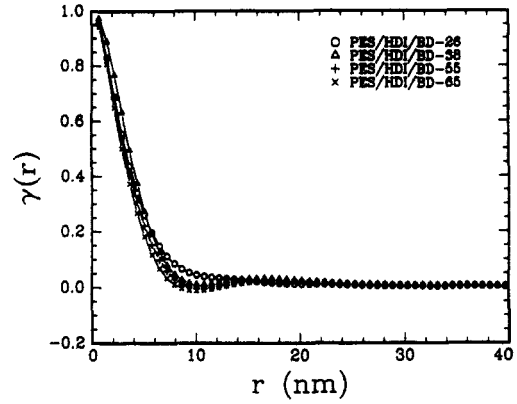

Figure 2. Three-dimensional correlation functions of PES/HDI/BD as-reacted samples. $\gamma(r) = \gamma_3(r)$.

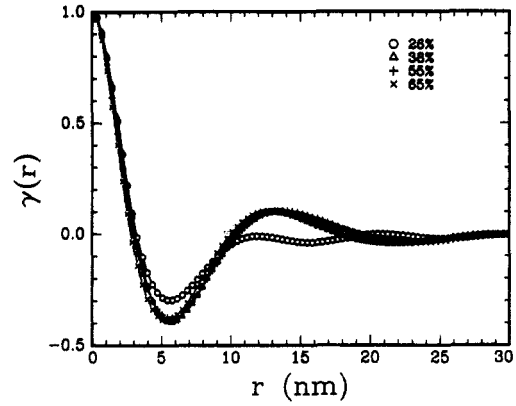

Figure 3. One-dimensional correlation functions of PES/HDI/BD as-reacted samples. $\gamma(r) = \gamma_1(r)$.

performed at the same temperature, irrespective of the phase structure of the samples. Therefore, the degrees of phase separation of the samples with different thermal treatments can be estimated and compared with each other by using the Q values on a relative scale (the absolute intensity calibration constant was not available during the time of our SAXS experiments). It is not necessary to use the absolute value of Q for comparison purposes in the present study.

The assumption of spherical symmetry is not valid for many cases. For example, the lamellar structure could show local anisotropy. Then the normalized one-dimensional correlation function could be more appropriate[26]

$$\gamma_1(r) = (1/Q)\int_0^\infty q^2 I(q) \cos(qr)\, dq \qquad (4)$$

It should be noted that by defining the three- and the one-dimensional correlation functions in this way, the absolute intensity calibration is not needed.

In reality, due to instrument limitation in most cases, the scattered intensity curves are truncated at both ends. In this study, the low q end was made up by using the Debye–Bueche theory

$$I(q) = 8\pi\langle\eta^2\rangle l_p^3/[1 + l_p^2 q^2]^2 \qquad (5)$$

where l_p is an inhomogeneity length. An extension in the high-angle data was performed by using the Porod–Ruland theory[26,27]

$$\lim_{q\to\infty}[I(q)] = K_p/q^4 \exp(-\sigma^2 q^2) + I_B \qquad (6)$$

where K_p is a constant related to the surface-to-volume ratio of the phases, I_B is a constant related to the thermal fluctuations, and σ is related to the thickness of the interface E by

$$E \approx 12^{1/2}\sigma \qquad (7)$$

The interdomain spacing d can be approximated from the position of the primary maximum of the correlation function, if the one-dimension geometry is applicable. The other method uses the Bragg equation

$$d = 2\pi/q_m \qquad (8)$$

where q_m is the q value at the position of a maximum in the scattering curve. However, if the system contains randomly oriented lamellar structure, the random arrangement of the one-dimensional repeating structure has to be corrected by performing the so-called Lorentz correction, i.e., by multiplying the scattered intensity with q^2. Then the peak position is determined from a plot of $I(q)q^2$ versus q, instead of a plot of $I(q)$ versus q.

Figure 1 shows the SAXS patterns of as-reacted PES/HDI/BD samples. Except for PES/HDI/BD-26, all other curves show a peak. This is an indication of a two-phase structure. Figure 2 shows the corresponding three-dimensional correlation functions. The results suggest that the structure is not totally random due to the nonexponential decay. The interdomain spacing of PES/HDI/BD-38 is estimated to be 16.6 nm. Figure 3 shows the corresponding one-dimensional correlation functions. The main characteristic of the one-dimensional correlation function is that it showed periodicity, an indication of two-phase structure. The oscillation diminished very quickly, due to a broad distribution of the interdomain spacing. The interdomain spacing in PES/HDI/BD-38 is 13.0 nm. According to Figure 3, the interdomain spacing from the Bragg equation using a plot of Iq^2 versus q is 14.0 nm. In addition, the spherulite structure, implying the existence of the lamellar structure,[14] has been observed from the sample. Spherulite structures have also been observed from pure HDI/BD homopolymers.[28,29] Therefore the one-dimensional correlation function analysis seems to be more appropriate for the systems under study. Figure 4 shows the dependence of the interdomain spacing on the hard-segment content as determined from the one-dimensional correlation functions. Although the hard-segment content was increased from 26 to 65%, corresponding to a molar ratio of PES:HDI:BD = 1:3:2 to 1:15:14, the interdomain spacing shows very little change. It even decreased for the as-reacted PES/HDI/BD-65 sample.

Figure 5 shows SAXS patterns of the PES/HDI/BD samples after the sample melts (188 °C) were quenched to 135 °C and annealed for 24 h. The two-phase structure is obvious from the scattering maximum of each curve. The scattering curves, however, do not show a significant difference. This is obvious from their corresponding one-dimensional correlation functions, as shown in Figure 6. Once again, the interdomain spacing showed very little

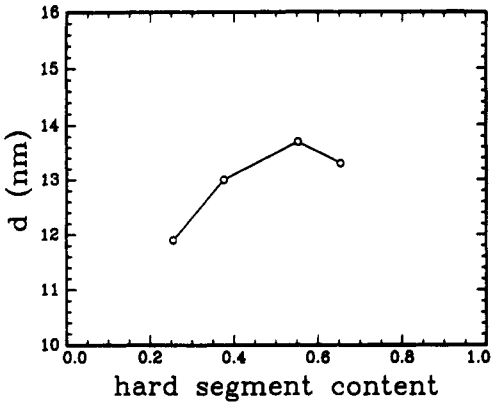

Figure 4. Dependence of interdomain spacing upon hard-segment content for PES/HDI/BD as-reacted samples. The interdomain spacing values were obtained from the first nonzero maximum of the one-dimensional correlation function.

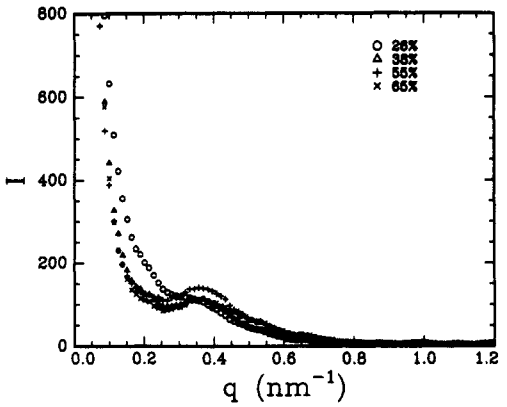

Figure 5. SAXS patterns of PES/HDI/BD. The samples were melted at 188 °C and quenched to an annealing temperature at 135 °C and annealed for 24 h.

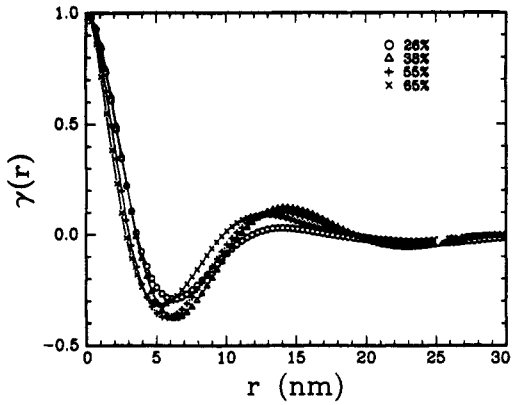

Figure 6. One-dimensional correlation functions of PES/HDI/BD. The samples were melted at 188 °C and quenched to an annealing temperature of 135 °C and annealed for 24 h.

change with increasing hard-segment content, suggesting that the HDI/BD hard-segment chains were in a folded-chain conformation. The Koberstein–Stein coiled/folded chain model for MDI/BD hard-segment chains could be applied to the HDI/BD system.

Although there are few reports on HDI/BD-based segmented polyurethanes,[14] extensive studies have been reported on the pure HDI/BD homopolymer. Kern et al.[30] found that for oligomers of HDI/BD, $HO(CH_2)$-$[OCONH(CH_2)_6NHCOO(CH_2)_4]_xOH$, the lamellar thickness of the crystal grown from solution is proportional to the molecular length up to $x = 5$. At $x > 5$, the lamellar thickness remained essentially unchanged, indicating chain folding. Interestingly, here we observed an insensitivity of interdomain spacing with increasing hard-segment

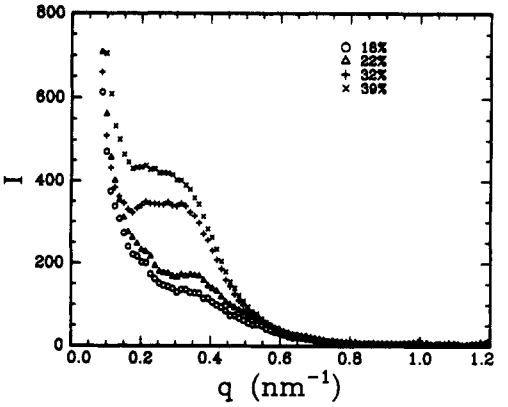

Figure 7. SAXS patterns of PES/MDI/DDE solution-cast samples.

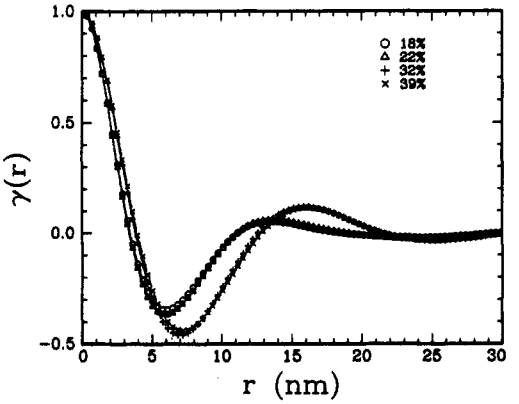

Figure 8. One-dimensional correlation functions of PES/MDI/DDE solution-cast samples.

length, implying that the chain-folding feature of HDI/BD remained in the HDI/BD-based segmented polyurethanes.

Now we turn to the PES/MDI/DDE series, where the MDI/DDE hard segments are more rigid and the interaction between the hard segments is stronger due to the urea group. Figure 7 shows SAXS patterns of the PES/MDI/DDE samples. A significant increase in the scattered intensity was observed with increasing hard-segment content. The interdomain spacing increased with increasing hard-segment content, as shown in Figure 8, which is totally different from the PES/HDI/BD series. We believe that the MDI/DDE hard segments probably did not adopt the folded-chain conformation as the PES/HDI/BD samples, although a coiled-chain conformation could be possible. Also the results could not rule out the possibility of an extended-chain conformation.

Similar phenomena were observed for the PTMO/MDI/DDE series (Figures 9 and 10). Unfortunately, the interactions between the MDI/DDE hard segments were so strong that a melt could not be obtained without thermal decomposition. It was not possible to study in detail the thermal effects on the phase structure of MDI/DDE samples. In addition, the MDI/DDE-based segmented polyurethane samples were not stable against high-temperature annealing. Therefore annealing experiments were not performed.

It should be interesting to compare the interdomain spacing of the three series. From Figure 11, we can clearly see the dependence of interdomain spacing upon the hard-segment content for the three series. Samples based on MDI/DDE show significant increase with increasing hard-segment content while samples based on HDI/BD do not.

It was observed that the interdomain spacing of MDI/BD-based segmented polyurethanes increased with in-

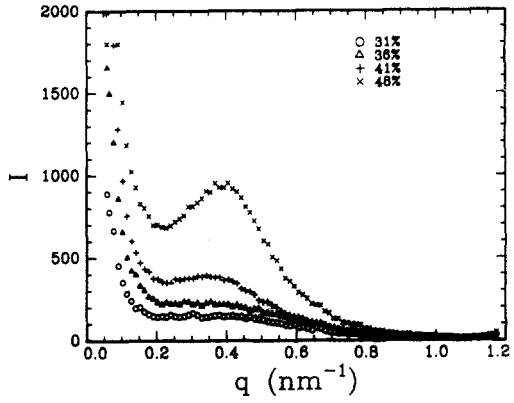

Figure 9. SAXS patterns of PTMO/MDI/DDE solution-cast samples.

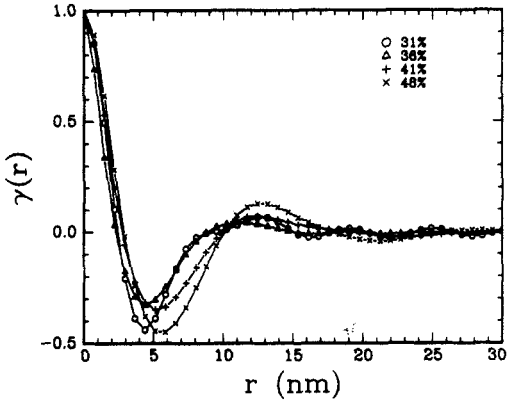

Figure 10. One-dimensional correlation functions of PTMO/MDI/DDE solution-cast samples.

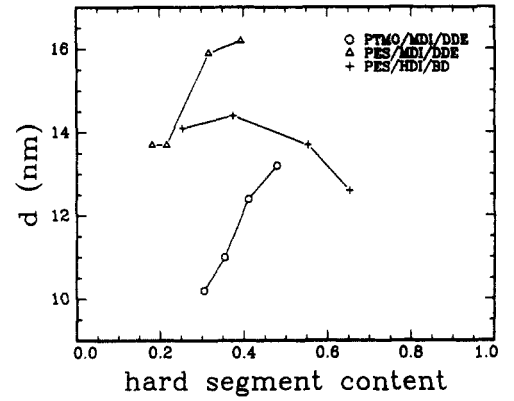

Figure 11. Dependence of interdomain spacing upon hard-segment content for the three classes of segmented polyurethanes. Samples of PES/MDI/DDE and PTMO/MDI/DDE were solution-cast, and samples of PES/HDI/BD were prepared by being melted at 188 °C, quenched to 135 °C, and annealed for 24 h. The interdomain spacing values were obtained from the first nonzero maximum of the corresponding one-dimensional correlation functions.

creasing annealing temperature.[5] The SAXS patterns of PES/HDI/BD-26 and PES/HDI/BD-38 under different annealing conditions are shown in Figures 12 and 14, and their corresponding one-dimensional correlation functions, in Figures 13 and 15, respectively. The interdomain spacing shows very little increase with increasing annealing temperature (Figure 16). The invariant increased slightly, indicating the phase perfection with increasing annealing temperature, as shown in Figure 17.

To better understand the effects of thermal treatments on the phase structure, the phase separation kinetics was followed after the sample melts were quenched to 25, 80, and 135 °C. The phase separation kinetics results shown

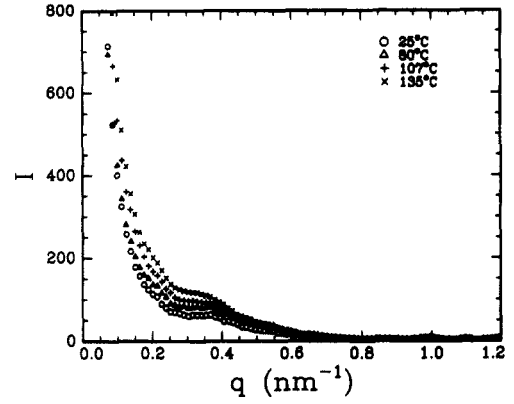

Figure 12. SAXS patterns of PES/HDI/BD-26 melted at 188 °C, quenched to different annealing temperatures, and annealed for 24 h.

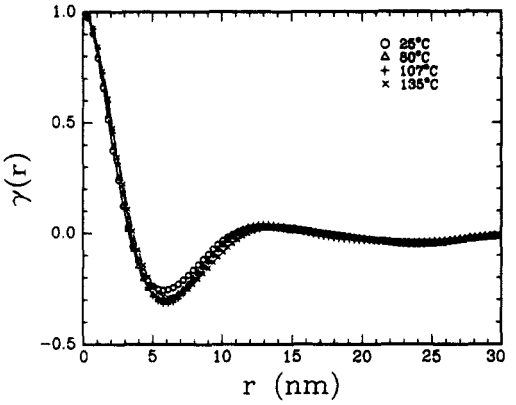

Figure 13. One-dimensional correlation functions of PES/HDI/BD-26 melted at 188 °C, quenched to different annealing temperatures, and annealed for 24 h.

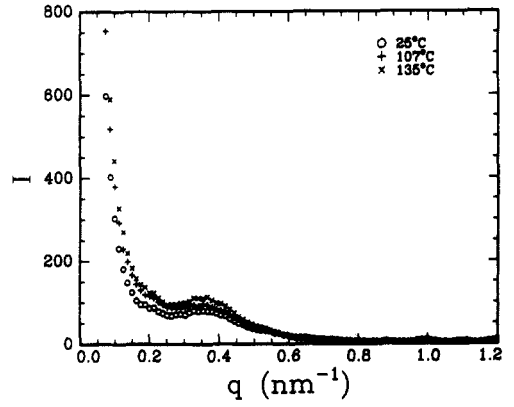

Figure 14. SAXS patterns of PES/HDI/BD-38 melted at 188 °C, quenched to different annealing temperatures, and annealed for 24 h.

in Figure 18 indicated that the phase separation was very fast. The phase separation was accomplished in about 1–2 min at annealing temperatures from 25 to 135 °C. A quantitative description of the phase separation kinetics was not possible due to instrument limitation and the fact that it took about 20–30 s for the samples to be cooled to the desired annealing temperatures. In a previous study, we observed a fast spherulite growth.[14] On the other hand, our phase separation kinetics study of a MDI/BD-based segmented polyurethane showed that the phase separation was accomplished in hours at most of the annealing temperatures.[6] The fast phase separation in PES/HDI/BD samples obviously resulted from the high mobility of HDI/BD hard segments and the low system viscosity. Unfortunately, the rapid phase separation also created an experimental difficulty as the phase separation could take

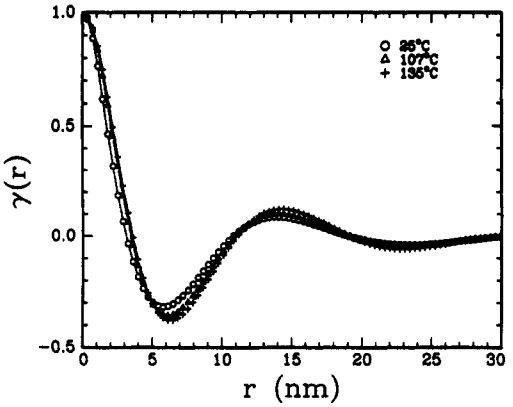

Figure 15. One-dimensional correlation functions of PES/HDI/BD-38 melted at 188 °C, quenched to different annealing temperatures, and annealed for 24 h.

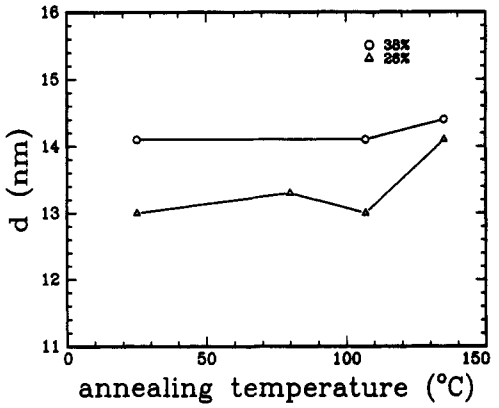

Figure 16. Dependence of interdomain spacing upon annealing temperature for PES/HDI/BD with different hard-segment content. The samples were prepared by being melted at 188 °C, quenched to different annealing temperatures, and annealed for 24 h. The interdomain spacing was obtained from the first nonzero maximum of the correlation function.

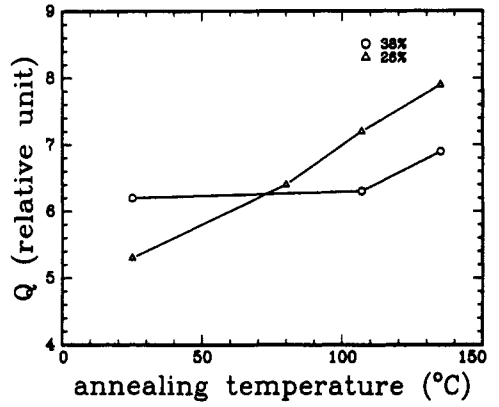

Figure 17. Dependence of invariant, Q, upon the annealing temperature for PES/HDI/BD-26 and PES/HDI/BD-38.

place during a cooling process. Then the anticipated annealing process became a kind of postannealing process. This rapid phase separation was partially responsible for the insensitivity of the annealing process at different temperatures because the main effect took place during the cooling process and the structure was locked in before the annealing temperature was reached. Furthermore, it could also explain why postannealing had little effect. The fact that annealing temperatures could not alter the structures appreciably also suggested that the interactions among the hard-segment chains were very strong and the strong interactions prevented the hard segments from being taken apart. This argument agrees well with the results from MDI/BD-based segmented polyurethanes.

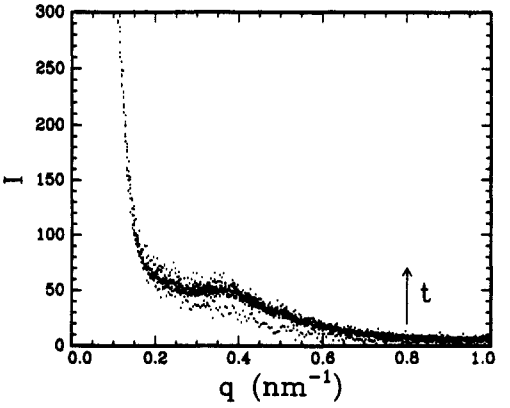

Figure 18. Time dependence of SAXS behavior of PES/HDI/BD-55. The sample was melted at 188 °C. The elapsed time was counted after the melt was jumped to 80 °C. The SAXS patterns were recorded at 27, 92, 155, 218, 294, 481, 738, 1126, and 1607 s. The bottom curve was recorded at 27 s. All other curves overlapped, indicating that the phase separation took place within the first 1–2 min.

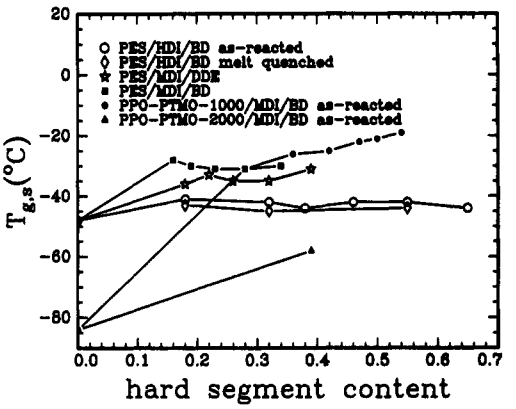

Figure 19. $T_{g,s}$ values as a function of hard-segment content based on DSC thermograms of the segmented polyurethanes.

Once the system reached equilibrium and a certain degree of interaction, postannealing had very little effect.[8]

(2) DSC Results. Figure 19 shows the glass transition temperatures of the soft-segment phase ($T_{g,s}$) for the four series of segmented polyurethane samples from the DSC measurements. It was expected that the use of aliphatic diisocyanate (HDI) would decrease the incompatibility between the hard and soft segments (Table I). Surprisingly, the $T_{g,s}$ values of the PES/HDI/BD series were only about 5 °C above that of the pure soft-segment oligomer PES ($T_{g,s,0}$). The fact that $T_{g,s} > T_{g,s,0}$ could partially be due to the restriction from the hard-segment domains where the two soft-segment ends were anchored and partially be due to the presence of hard segments in the soft-segment phase. Camberlin and Pascault[31] showed that the chain end restriction would raise the $T_{g,s}$ by about 4 °C. As our system had a soft-segment molecular weight of 2000 when compared with their 2280, our results indicated that the phase separation in the PES/HDI/BD samples was nearly complete. By replacing MDI with HDI, we expected a decrease in the thermodynamic incompatibility between the soft and the hard segments (Table I). The DSC results suggested that the thermodynamic factor was not important.

It was also expected that the introduction of the urea group would increase the incompatibility between the hard and soft segments (Table I). The $T_{g,s}$ values of the PES/MDI/DDE samples were found to be indeed lower than those of the PES/MDI/BD samples. But they were higher than those of the PES/HDI/BD samples by about 10 °C. Therefore the $T_{g,s}$ values could not be explained success-

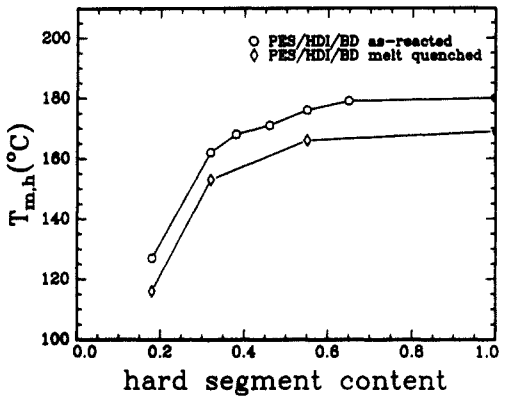

Figure 20. $T_{m,h}$ values as a function of hard-segment content based on DSC thermograms of the segmented polyurethanes.

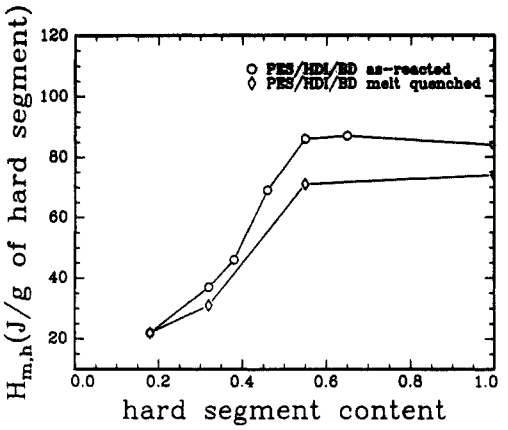

Figure 21. $H_{m,h}$ values as a function of hard-segment content based on DSC thermograms of the segmented polyurethanes.

fully by using only the thermodynamic principles. The kinetic factor has to be considered and is discussed in more detail in the following section.

The $T_{g,s}$ values from the PES/HDI/BD samples prepared by quenching the sample melts to about −160 °C were very close to those of the as-reacted samples. Therefore DSC results also showed that the phase separation in the PES/HDI/BD samples was very rapid.

Due to the symmetry and flexibility of the HDI/BD hard segment, crystallization was observed in DSC thermograms. The melting temperatures ($T_{m,h}$) are shown in Figure 20 as a function of the hard-segment content. The heat of fusion ($H_{m,h}$) is given in Figure 21 as a function of the hard-segment content. $T_{m,h}$ and $H_{m,h}$ increased with increasing hard-segment content up to about 50%. Further increase in the hard-segment content showed little effect on the $T_{m,h}$ and $H_{m,h}$ values. Actually, a small decrease in $H_{m,h}$ was observed when the hard-segment content was increased from 65 to 100% for the as-reacted PES/HDI/BD samples. The $T_{m,h}$ value of the pure HDI/BD hard segment was 180 °C, in agreement with the result by MacKnight et al.[32] (182 °C), while the $H_{m,h}$ value, 84 J/g, was higher than their 70 J/g. Melt-quenched samples also showed obvious crystallization, an indication of fast phase separation, although the corresponding $T_{m,h}$ and $H_{m,h}$ values were lower. MacKnight et al.[32] also estimated that the heat of fusion for 100% crystalline HDI/BD hard segment should be close to 189 J/g, that of Nylon 66. Then we could see that the crystallinity of the HDI/BD hard-segment domains in the as-reacted samples was increased from ~12% (PES/HDI/BD-26) to ~46% (PES/HDI/BD-55 and -65). Further increase in the hard-segment content gave rise to a slight decrease to ~44% for pure HDI/BD. This could readily be explained by a folded-chain conformation of the hard segments. Interestingly, similar $T_{m,h}$ and $H_{m,h}$ versus hard-segment content relationships were also reported by Leung and Koberstein[4] for their MDI/BD-based samples where the MDI/BD hard segments were claimed to be in the coiled/folded chain conformation.

No melting peak was observed for the MDI/DDE-based samples before thermal decomposition took place at about 220 °C in air.

(3) More Discussion on $T_{g,s}$. The synchrotron SAXS results and the DSC results on the $T_{g,s}$ values shown in the preceding sections should remind us that there exists a very interesting controversy in segmented polyurethanes. The theoretical work by Krause[33] showed that in a block copolymer, if the length of one of the blocks was increased, the incompatibility between the two blocks was increased. Experimentally, a previous study[34] and our DSC results on the PPO–PTMO/MDI/BD samples (Figure 19) showed that if the soft-segment length in a segmented polyurethane was increased, the ($T_{g,s}$ − $T_{g,s,0}$) value was decreased, implying that fewer hard segments existed in the soft-segment phase, in agreement with the theory. However, if the hard-segment content (length) were increased, the results were very controversial and depended upon many factors such as the chemical structure of the two segments, the soft-segment length, and the conditions of sample preparation. To our knowledge, there has been no explanation for this obvious controversy. Some of the main features are discussed as follows.

1. Figure 19 showed that as the hard-segment content was increased in PPO–PTMO-1000/MDI/BD, the ($T_{g,s}$ − $T_{g,s,0}$) values were increased, suggesting that *more* hard segments existed in the soft-segment phase, in direct conflict with the theory. This phenomenon was also observed by other groups from the following samples: as-reacted, compression molded, or solution cast; polyester or polyester as soft segment; MDI, TDI, 4,4′-methylenebis-(cyclohexyl isocyanate) (HMDI) or piperazine with BD as hard segment; monodisperse or polydisperse hard-segment length distribution.[11,35-39] Similar phenomena were also observed in poly(ether–ester) segmented copolymers.[35]

2. Figure 19 showed that if the soft segment had a molecular weight of ~2000, the deviation from the theory was less serious. The scale of changes in the $T_{g,s}$ values was smaller and the $T_{g,s}$ values were closer to the $T_{g,s,0}$ values, when compared with their 1000 g/mol molecular weight analogs, implying that fewer hard segments exist in the soft-segment phase. A literature search revealed that an increase (or no significant changes) in the $T_{g,s}$ values was observed with increasing hard-segment content if polyesters, poly(propylene oxide) (PPO), or PPO end-capped with poly(ethylene oxide) (PEG–PPO–PEO) were used as the soft segments;[4,11,35,41-43] a decrease in the $T_{g,s}$ values was observed with increasing hard-segment content if PTMO was used as the soft segment.[40,44] The samples used include soft-segment length ≈ 2000 g/mol or higher; as-reacted, compression molded, or solution cast; polyester or polyether as soft segment; MDI, TDI, or HMDI with BD as hard segment; and monodisperse or polydisperse hard-segment length distribution. In particular, if polybutadiene (PBD), polyisobutylene (PIB), or poly(dimethylsiloxane) (PDMSO) were used as the soft segment and MDI, or TDI, with BD as the hard segment,[45-48] no significant changes in the $T_{g,s}$ values were observed with increasing hard-segment content. The $T_{g,s}$ values were very close to the $T_{g,s,0}$ values, implying that very few hard segments were present in the soft-segment phase. Thermal treatment showed very little effect on the $T_{g,s}$ values.

3. Figure 19 showed that if aliphatic diisocyanate HDI was used to replace aromatic diisocyanate MDI, no significant changes in the $T_{g,s}$ values were observed with increasing hard-segment content. The $T_{g,s}$ values were very close to the $T_{g,s,0}$ values. Similar results have also been reported before for other aliphatic diisocyanates.[10,11,15,35]

4. Figure 19 and previous studies[20,40,49] showed that if diamines were used to replace BD as chain extenders, a slight decrease, a slight increase, or no significant changes in the $T_{g,s}$ values were observed with increasing hard-segment content. The $T_{g,s}$ values were close to the $T_{g,s,0}$ values. Thermal treatment showed little effect.

The controversy between the theory and the experimental results cannot be reconciled by the polydispersity of the hard-segment length distribution because samples with monodisperse hard-segment length distribution showed similar phenomena.[39,41]

The phase-separated structure of segmented polyurethanes depended upon how the samples were prepared. In particular, we observed that the phase structure was not irreversible against thermal annealing. As the conditions of sample preparation became a dominant factor, the experimental results also depended upon sample preparation. In compression molding, solution casting, or bulk polymerization of segmented polyurethane samples, the initial condition was that the system was homogeneous. Phase separation could take place later due to changes in temperature, concentration, or segment length. There could be two controlling factors for the phase separation, i.e., the thermodynamic factor and the kinetic factor. Thermodynamic incompatibility only ensures whether phase separation would occur, while the kinetic factor could control the actual occurrence of phase separation. In previous investigations, much attention was paid to the thermodynamic factor, although time dependence studies indicated that the phase separation process was not rapid in most cases. By using DSC, mechanical test, and SAXS, Wilkes and co-workers[50] found that the phase separation process in their samples could take as long as days. Slow phase separation behavior was also observed by Kwei,[51] Camberlin and Pascault,[52] and Lee et al.[53] Galambos et al.[54] used synchrotron SAXS and WAXD to study the phase separation and crystallization kinetics of their segmented polyurethanes with a soft-segment molecular weight of ~2000. Comparatively shorter time periods of tens of minutes were required to complete the phase separation process. By using synchrotron SAXS, we found that the microphase structural development in a segmented polyurethane based on MDI/BD was very slow.[6] The phase separation process could be described by a relaxation equation. The system viscosity, the hard-segment mobility, and the interactions among hard segments were three controlling factors. We believe that the viscosity–mobility–interaction argument could be used to explain the controversy in the relationship between $T_{g,s}$ and the hard-segment content.

The Cahn–Hilliard–Cook–Binder theory[55] could be used to reveal some qualitative guidance. For a two-component system undergoing phase separation, the phase separation rate $R(q)$ can be expressed by

$$R(q) = -Mq^2\left[\frac{\partial^2 f}{\partial \phi_0^{\,2}} + 2Kq^2\right] = -D_{app}q^2 - 2MKq^4 \quad (9)$$

where D_{app} is an apparent diffusion coefficient, M is the mobility, $\partial^2 f/\partial \phi_0^2$ is the second derivative of free energy of mixing with respect to composition ϕ_0, and K is the interfacial free energy density. It should be emphasized that eq 9 is valid for two-component systems like polymer blends and is being used here to provide us with some qualitative guidance.

Equation 9 implies that in a segmented polyurethane, the phase separation rate is directly related to the hard-segment mobility. Furthermore, from the Stokes–Einstein equation, the diffusion coefficient is also related to the soft-segment viscosity. Our SAXS studies[6] showed that a decrease in the phase separation rate could be expected with either decreasing hard-segment mobility or increasing soft-segment viscosity. The hard-segment mobility depends partially upon the flexibility of the hard segment. The hard-segment mobility also increases with decreasing soft-segment viscosity.

The controversy between the theory and experimental results could be explained by a lack of equilibrium, due to *kinetic* effects. Generally, the system viscosity in a segmented polyurethane is high and the hard-segment mobility is low. There could be entanglement or hydrogen bonding between the hard and soft segments. Therefore the phase separation kinetics is not rapid in most cases. In the conditions of sample preparation reported previously, the samples might not be able to reach equilibrium. In particular, postannealing at room temperature might never complete the phase separation due to the high system viscosity and low hard-segment mobility, no matter how long the samples were stored in a desiccator before measurements. Hence, the $T_{g,s}$ values might be obtained from nonequilibration systems and could depend upon how far the systems were off from the equilibrium. Now consider the relationship between $T_{g,s}$ and the hard-segment content. Although thermodynamic incompatibility is increased with increasing hard-segment content, a purer soft-segment phase might not be realized due to the kinetic barrier. Actually, the hard-segment mobility is decreased with increasing hard-segment length or with increasing soft-segment viscosity. The deviation from equilibrium is increased with increasing hard-segment content, resulting in an increase in $T_{g,s}$, which accounts for the controversy between the theory and the experimental results.

If the soft-segment molecular weight was increased from ~1000 to ~2000 or higher, the surface-to-volume ratio of the hard-segment domains and the degree of connectivity between the hard and soft segments could consequently be decreased. Therefore the hard-segment domains could exert less restriction to the soft segments.[44] The soft segments became easier to move and to exclude the hard segments out of the soft-segment phase. The kinetic factor became less obvious, resulting in a smaller deviation from the theory. As PTMO has a very low viscosity,[52] the kinetic effects are no longer significant. So the dependence of $T_{g,s}$ upon hard-segment content agrees with the theory.[40,44] The same is also true when PBD, PIB, and PDMSO were used as the soft segments.[45-48] In particular, hydrogen bonds could not be formed between the hard and soft segments in PBD- and PIB-based segmented polyurethanes.

If the hard-segment mobility was increased by changing the chemical structure of the hard segments, the kinetic barrier could become less important. Our DSC results showed that with the soft segment remaining unchanged, the HDI/BD hard segment could reduce the $T_{g,s}$ values when compared with those using the aromatic diisocyanates (see also refs 10, 11, 15, and 35 for other aliphatic diisocyanates). Furthermore, our synchrotron SAXS and

DSC studies showed that the phase separation could be completed within a couple of minutes if HDI/BD was used as the hard segment. Thermal annealing showed little effect on the phase structure of the samples. Aitken and Jeffs[15] showed that the aliphatic diisocyanate based segmented polyurethanes had a stronger tendency to exist in two phases than the aromatic diisocyanate based segmented polyurethanes, even when an unsymmetrical aliphatic diisocyanate was used. For the latter case, the driving force for phase separation due to the hard-segment crystallization would be absent. This behavior suggests that the high mobility of aliphatic diisocyanates is the cause.

The following could be the reason why the thermodynamic factor was overemphasized in previous investigations. The hard segments used in segmented polyurethanes were usually very polar with high solubility parameters. Greater thermodynamic incompatibility could be obtained if the soft segments employed had smaller polarities (smaller solubility parameters). Thus, segmented polyurethanes with PBD, PIB, or PDMSO as the soft segments usually had $T_{g,s}$ values very close to the $T_{g,s,0}$ values. However, it should be noted that these soft segments also had relatively weak intermolecular forces which were partially responsible for the low $T_{g,s,0}$ values (and poorer mechanical properties). The viscosity was usually lower than that of polyesters, PEO–PPO–PEO or PPO–PTMO. Camberlin and Pascault[52] were able to show that the phase separation rate increased with decreasing viscosity of the soft segments or with increasing ΔT based on the Doolittle equation, where $\Delta T = 298 - T_{g,s,0}$. Therefore in segmented polyurethanes with PBD, PIB, or PDMSO as the soft segments, both thermodynamic and kinetic factors favor phase separation. While the thermodynamic factor could be used to explain the phenomena in PBD-, PIB-, or PDMSO-based segmented polyurethanes where the kinetic factor did not play a major role, it would run into trouble if the soft segments had a molecular weight of 1000 or if the polyesters PEO–PPO–PEO with a molecular weight of 2000 were used as the soft segments. Under those conditions, the kinetic factor would dominate.

Supposing the above statements are true, one would expect that the kinetic effect should be more important in compression molded or reaction injection molded samples and should be reduced by using the solution-casting method in specimen preparation, where longer preparation time and lower system viscosity are usually involved. Furthermore, the reduction of kinetic effects should be more obvious for segmented polyurethanes with higher hard-segment content (lower mobility). The solution-cast samples should also show lower $T_{g,s}$ values when compared with those from compression molding since the phase separation in solution-cast samples should be closer to equilibrium. Experimentally, these phenomena have been observed by Schneider et al.[36] and Willkomm et al.[20]

The introduction of diamines in replacement of BD as the chain extender strongly increases the self-cohesive ability of the hard segments. If the samples were prepared from solution, the controversy between the theory and the experimental results would be less obvious, as shown in Figure 19 and refs 40 and 49. However, reaction injection molded samples with hard segment based on MDI and diethyltoluenediamine (lower mobility of hard segment) shows a slight increase in $T_{g,s}$ with increasing hard-segment content, in conflict with the theoretical prediction, as expected.[20]

It could also be interesting to discuss the effects of increasing hard-segment content based on the characteristics of the hard-segment domains. However, in practice, there are several problems with it. (1) The glass transition temperature of the hard-segment domains ($T_{g,h}$), or the melting temperature of the ordered hard-segment domains could not always be observed. (2) The hard-segment length polydispersity effects are more important.[56] (3) The effects of sample preparation and thermal history are even more significant for the hard-segment domains than for the soft-segment phase.[1,5,7,8,51,54,57–69] Therefore samples prepared from different groups might not be able to be compared. We believe that it should be easier to discuss the effects based on $T_{g,s}$.

The viscosity–mobility–interaction argument could also be used to explain the annealing effects on the phase-separated structure of segmented polyurethanes.[5] According to Koberstein,[68] the short hard segments become soluble in the soft-segment phase. Therefore, thermodynamically the most complete phase separation should take place in those samples annealed at lower temperatures. However, our studies showed that the most complete phase separation took place at ~107 °C for PPO–PTMO–1000/MDI/BD. From the kinetic viewpoint, the phase separation process could not be complete because of the high system viscosity at lower temperatures. As the annealing temperature is increased, the system viscosity is decreased and the hard segments gain more mobility. Then the kinetic barrier becomes less important. Thus more complete phase separation takes place at ~107 °C. As the annealing temperature is further increased, the decrease in the thermodynamic incompatibility becomes more important while the kinetic barrier becomes even less important. The degree of phase separation is decreased.

In summary, the controversy between theory and experimental results on the relationship between $T_{g,s}$ and hard-segment content could be explained by the viscosity–mobility–interaction argument. The importance of the kinetic factor should always be considered seriously. The phase-separated structure in segmented polyurethanes is often not at equilibrium, being quenched from the homogeneous state with the phase-separated structure frozen at some nonequilibrium state depending on the cooling rate, the hard-segment mobility, and the system viscosity. At room temperature the system viscosity in most segmented polyurethanes based on MDI/BD or TDI/BD and polyesters is so high that phase separation is hindered and the system could not reach an equilibrium state at that temperature. High-temperature annealing could improve phase separation. However, it has to be noted that at high temperatures, the thermodynamic factor becomes more important and short hard segments can be dissolved in the soft-segment phase due to decreasing thermodynamic incompatibility between the hard segment and the soft segment, although these short hard segments are thermodynamically insoluble at room temperatures.

Since this study is involved with several series of segmented polyurethane samples prepared under a variety of conditions, a schematic flow chart is given in Chart I to clarify some of our main points. However, it has to be noted that the viscosity–mobility–interaction argument is obviously oversimplified. The structure–property relationships could be more complex than expected. Quantitative conclusions are difficult to obtain without further studies.

Summary of Some of the Main Points in This Study

1. Samples: Polyesters or Polyethers as Soft Segments with Molecular Weight $M_{n,s} \sim 1000$; MDI/BD, TDI/BD, HMDI/MD, Piperazine/BD, and Poly(tetramethylene terephthalate) (PTMT) as Hard Segments

Hard-segment mobility: low (compared with other aliphatic polymer systems)
System viscosity: high (compared with other aliphatic polymer systems with weak intermolecular forces)
Thermodynamic prediction: high degree of phase separation (DPS) (solubility parameters of the soft and hard segments are generally substantially different)
Kinetic prediction: not as high as that by thermodynamic prediction
$(T_{g,s} - T_{g,s,0})$ experiment: DPS not as high as that by thermodynamic prediction
$T_{g,s} \sim W_h$ (hard-segment content) obeys Krause theory? no

2. Samples: $M_{n,s}$ Increased to ~2000

Hard-segment mobility: increased (easier to be excluded from soft-segment phases)
Thermodynamic prediction: higher DPS
Kinetic prediction: higher DPS
$(T_{g,s} - T_{g,s,0})$ experiment: higher DPS
$T_{g,s} \sim W_h$ obeys Krause theory? from yes to not obvious

3. Samples: PBD, PIB, and PDMSO as Soft Segments

Hard-segment mobility: increased
System viscosity: low
Thermodynamic prediction: higher DPS
Kinetic prediction: higher DPS
$(T_{g,s} - T_{g,s,0})$ experiment: higher DPS
$T_{g,s} \sim W_h$ obeys Krause theory? yes

4. Samples: Aliphatic Hard Segments

Hard-segment mobility: increased
Thermodynamic prediction: lower DPS
Kinetic prediction: higher DPS
$(T_{g,s} - T_{g,s,0})$ experiment: higher DPS
$T_{g,s} \sim W_h$ obeys Krause theory? yes

5. Samples: Diamines as Chain Extenders

Hard-segment mobility: depends
Additional factor: strong cohesive force due to urea groups
Thermodynamic prediction: higher DPS
Kinetic prediction: depends
$(T_{g,s} - T_{g,s,0})$: higher DPS
$T_{g,s} \sim W_h$ obeys Krause theory? depends on sample preparation

6. Samples: Prepared from Solution

Hard-segment mobility: increased
System viscosity: decreased
Thermodynamic prediction: DPS basically unchanged
Kinetic prediction: higher DPS
$(T_{g,s} - T_{g,s,0})$ experiment: higher DPS
$T_{g,s} \sim W_h$ obeys Krause theory? from yes to not obvious

7. Samples: Upon Annealing

Hard-segment mobility: increased with increasing annealing temperature (T_A)
System viscosity: decreased with increasing T_A
Thermodynamic prediction: decreased DPS with increasing T_A
Kinetic prediction: increasing DPS with increasing T_A
DPS from SAXS experiment: DPS increased first with increasing T_A and reached a maximum (~107 °C for PPO–PTMO-1000/MDI/BD-50); further increase in T_A caused a decrease in DPS

IV. Concluding Remarks

To test our viscosity–mobility–interaction concept, a few series of segmented polyurethanes were synthesized which have different hard-segment flexibilities and interactions. All the synchrotron SAXS and DSC results could be explained by the viscosity–mobility–interaction argument and once again showed that kinetic effects should be considered in the structure–property relationships of segmented polyurethanes. The PES/HDI/BD systems have low system viscosity, high hard-segment mobility, and strong interaction between the hard-segment chains. The phase separation is rapid and the kinetic barriers are not important. The two MDI/DDE systems have high system viscosity, low hard-segment mobility, and strong interaction between the hard-segment chains. The kinetic effects are more important than HDI/BD-based segmented polyurethanes but less important than MDI/BD-based segmented polyurethanes. While the HDI/BD hard segments adopt a folded-chain configuration, the MDI/DDE hard segments most likely exist in coiled configurations. However, our results could not rule out the possibility of an extended MDI/DDE hard-segment conformation. Finally, a long-time controversy in this field could also be explained by the viscosity–mobility–interaction argument.

Acknowledgment. B.C. acknowledges the financial support of this project by the U.S. Department of Energy (Contract DEFG0286ER45237A005). We thank Prof. J. Liu, Mr. T. Gao, Drs. A. Darovsky, and Y. Gao, and Mr.

W. Lehnert for experimental assistance. We also thank Prof. Q. Ying and Dr. C. R. Desper for helpful discussions.

References and Notes

(1) Gibson, P. E.; Vallence, M. A.; Cooper, S. L. In *Developments in Block Copolymers*—1; Goodman, I., Ed.; Elsevier: London, 1982.
(2) Bonart, R.; Morbitzer, L.; Hentze, G. *J. Macromol. Sci., Phys.* **1969**, *B3* (2), 337.
(3) Koberstein, J. T.; Stein, R. S. *J. Polym. Sci., Polym. Phys. Ed.* **1983**, *21*, 1439.
(4) Leung, L. M.; Koberstein, J. T. *J. Polym. Sci., Polym. Phys. Ed.* **1985**, *23*, 1883.
(5) Li, Y.; Liu, J.; Yang, H.; Ma, D.; Chu, B. *Polym. Mater. Sci. Eng.* (*Proc. Am. Chem. Soc., Div. Polym. Mater. Sci. Eng.*) **1991**, *65*, 297.
(6) Li, Y.; Gao, T.; Chu, B. *Macromolecules* **1992**, *25*, 1737.
(7) Chu, B.; Li, Y. *Colloid Polym. Sci.*, accepted.
(8) Li, Y.; Gao, T.; Liu, J.; Linliu, K.; Desper, C. R.; Chu, B. *Macromolecules*, accepted.
(9) Mennicken, G. J. *Oil Colours Chem. Assoc.* **1966**, *49*, 639.
(10) Dieter, J. W.; Byrne, C. A. *Polym. Eng. Sci.* **1987**, *27*, 673.
(11) Van Bogart, J. W. C.; Gibson, P. E.; Cooper, S. L. *J. Polym. Sci., Polym. Phys. Ed.* **1983**, *21*, 65.
(12) Wong, S. W.; Frisch, K. C. *Adv. Urethane Sci. Technol.* **1981**, *8*, 75.
(13) Castro, A. J.; Hentschelm, P.; Brodoski, W.; Plummer, T. *J. Elast. Plast.* **1985**, *17*, 238.
(14) Ren, Z.; Ma, D.; Zhu, Y.; Yu, S.; Yang, H. *Chinese J. Appl. Chem.* **1988**, *5*, 54.
(15) Aitken, R. R.; Jeffs, G. M. F. *Polymer* **1977**, *18*, 197.
(16) Chang, Y. J. P.; Wilkes, G. L. *J. Polym. Sci., Polym. Phys. Ed.* **1975**, *13*, 455.
(17) Camberlin, Y.; Pascault, J. P.; Letoffe, M.; Claudy, P. *J. Polym. Sci., Polym. Chem. Ed.* **1982**, *20*, 1445.
(18) Kimura, I.; Ishihara, H.; Ono, H.; Yoshihara, N.; Nomura, S.; Kawai, H. *Macromolecules* **1974**, *7*, 355.
(19) Chen, Z. S.; Yang, W. P.; Macosko, C. W. *Rubber Chem. Technol.* **1988**, *61*, 86.
(20) Willkomm, W. R.; Chen, Z. S.; Macosko, C. W.; Gobran, D. A.; Thomas, E. L. *Polym. Eng. Sci.* **1988**, *28*, 888.
(21) Casey, J. P.; Milligan, B.; Fasolka, M. J. *J. Elast. Plast.* **1985**, *17*, 218.
(22) Ryan, A. J.; Stanford, J. L.; Still, R. H. *Br. Polym. J.* **1988**, *20*, 77.
(23) Ryan, A. J.; Stanford, J. L.; Wilkinson, A. N. *Polym. Bull.* **1987**, *18*, 517.
(24) Chu, B.; Wu, D.; Wu, C. *Rev. Sci. Instrum.* **1987**, *58*, 1158.
(25) Wu, D. Ph.D. Thesis, SUNY at Stony Brook, 1990.
(26) *Small Angle X-ray Scattering*; Glatter, O., Kratky, O., Eds.; Academic Press: London, 1983.
(27) Ruland, W. *J. Appl. Crystallogr.* **1971**, *4*, 70.
(28) Brenschede, W. *Kolloid Z.* **1949**, *114*, 35.
(29) Jenckel, E.; Klein, E. *Kolloid Z.* **1950**, *118*, 86.
(30) Kern, W.; Davidovits, J.; Rauterkus, K. J.; Schmidt, G. F. *Makromol. Chem.* **1961**, *43*, 106.
(31) Camberlin, Y.; Pascualt, J. P. *J. Polym. Sci., Polym. Chem. Ed.* **1983**, *21*, 415.
(32) MacKnight, W. J.; Yang, M.; Kajiyama, T. *Polym. Prepr.* (*Am. Chem. Soc., Div. Polym. Chem.*) **1968**, *9*, 860. Kajiyama, T.; MacKnight, W. J. *Polym. J.* **1970**, *1*, 548.
(33) Krause, S. In *Block Copolymers and Graft Copolymers*; Burke, J. J., Weiss, V., Eds.; Syracuse University Press: Syracuse, NY, 1973; p 143.
(34) Seefried, C. G., Jr.; Koleske, J. V.; Critchfield, F. E. *J. Appl. Polym. Sci.* **1975**, *19*, 2493.
(35) Van Bogart, J. W. C.; Lilaonitkul, A.; Lerner, L. E.; Cooper, S. L. *J. Macromol. Sci., Macromol. Sci., Phys.* **1980** *B17* (2), 267.
(36) Schneider, N. S.; Paik Sung, C. S.; Matton, R. W.; Illinger, J. L. *Macromolecules* **1975**, *8*, 62.
(37) Seefried, C. G., Jr.; Koleske, J. V.; Critchfield, F. E. *J. Appl. Polym. Sci.* **1975**, *19*, 2503.
(38) Srichatrapimuk, V. W.; Cooper, S. L. *J. Macromol. Sci., Phys.* **1978**, *B15* (2), 267.
(39) Ng, H. N.; Allegrezza, A. E.; Seymour, R. W.; Cooper, S. L. *Polymer* **1973**, *14*, 255.
(40) Paik Sung, C. S.; Hu, C. B.; Wu, C. S. *Macromolecules* **1980**, *13*, 111. Schneider, N. S.; Paik Sung, C. S. *Polym. Eng. Sci.* **1977**, *17*, 73.
(41) Christenson, C. P.; Harthcock, M. A.; Meadows, H. L.; Spell, W. L.; Howard, W. L.; Creswick, M. W.; Guerra, R. E.; Turner, R. B. *J. Polym. Sci., Polym. Phys. Ed.* **1986**, *24*, 1401.
(42) Seefried, C. G., Jr.; Koleske, J. V.; Critchfield, F. E. *J. Appl. Polym. Sci.* **1975**, *19*, 3185.
(43) Spathis, G.; Kontou, E.; Kefalas, V.; Apekis, L.; Christodoulides, C.; Pissis, P.; Ollivon, M.; Quinquenet, S. *J. Macromol. Sci., Phys.* **1990**, *B29* (1), 31.
(44) Abouzahr, S.; Wilkes, G. L.; Ophir, Z. *Polymer* **1982**, *23*, 1077.
(45) Schneider, N. S.; Matton, R. W. *Polym. Eng. Sci.* **1979**, *15*, 1122.
(46) Bengtson, B.; Feger, C.; MacKnight, W. J.; Schneider, N. S. *Polymer* **1985**, *26*, 895.
(47) Speckhard, T. A.; Gibson, P. E.; Cooper, S. L.; Change, V. S.; Kennedy, J. P. *Polymer* **1985**, *26*, 55.
(48) Yu, X.; Nagarajan, M. R.; Grasel, T. G.; Gibson, P. E.; Cooper, S. L. *J. Polym. Sci., Polym. Phys. Ed.* **1985**, *23*, 2319.
(49) Wang, C. B.; Cooper, S. L. *Macromolecules* **1983**, *16*, 775.
(50) Wilkes, G. L.; Wildnauer, R. *J. Appl. Phys.* **1975**, *46*, 4148. Gilkes, G. L.; Emerson, J. A. *J. Appl. Phys.* **1976**, *47*, 4261.
(51) Kwei, T. K. *J. Appl. Polym. Sci.* **1982**, *27*, 2891.
(52) Camberlin, Y.; Pascault, J. P. *J. Polym. Sci., Polym. Phys. Ed.* **1984**, *22*, 1835.
(53) Lee, H. S.; Wang, Y. K.; MacKnight, W. J.; Hsu, S. L. *Macromolecules* **1988**, *21*, 270. Lee, H. S.; Hsu, S. L. *Macromolecules* **1989**, *22*, 1100.
(54) Galambos, A. F.; Russell, T. P.; Koberstein, J. T. *Polym. Mater. Sci. Eng.* (*Proc. Am. Chem. Soc., Div. Polym. Mater. Sci. Eng.*) **1989**, *61*, 359. Galambos, A. F. Ph.D. Thesis, Princeton University, 1989.
(55) Cahn, J. W.; Hilliard, J. E. *J. Chem. Phys.* **1958**, *28*, 258. Cahn, J. W. *J. Chem. Phys.* **1965**, *42*, 93. Cook, H. E. *Acta Metall.* **1970**, *18*, 297. Binder, K. *J. Chem. Phys.* **1983**, *79*, 6387. Strobl, G. R. *Macromolecules* **1985**, *18*, 558.
(56) Harrell, L. L., Jr. *Macromolecules* **1969**, *2*, 607.
(57) Wilkes, G. L.; Samuals, S. L.; Crystal, R. *J. Macromol. Sci., Phys.* **1974**, *B10*, 203.
(58) Chang, A. L.; Thomas, E. L. *Adv. Ser. Chem.* **1979**, *No. 176*, 31.
(59) Chang, A. L.; Briber, R. M.; Thomas, E. L.; Zdrahala, R.; Critchfield, F. E. *Polymer* **1982**, *23*, 1060.
(60) Briber, R. M.; Thomas, E. L. *J. Macromol. Sci., Phys.* **1983**, *B22*, 509.
(61) Seymour, R. W.; Cooper, S. L. *J. Polym. Sci., Polym. Lett. Ed.* **1971**, *9*, 689.
(62) Samuels, S. L.; Wilkes, G. L. *J. Polym. Sci., Polym. Lett. Ed.* **1973**, *11*, 807.
(63) Seymour, R. W.; Cooper, S. L. *Macromolecules* **1973**, *6*, 48.
(64) Jacques, C. H. M. In *Polymer Alloys: Blends, Blocks, Grafts, and Interpenetrating Networks*; Klempner, D., Frisch, K., Eds.; Plenum Press: New York, 1977; *Polymer Science and Technology*, Vol. 10, p 287.
(65) Hesketh, T. R.; Van Bogart, J. W. C.; Cooper, S. L. *Polym. Eng. Sci.* **1980**, *20*, 190.
(66) Van Bogart, J. W. C.; Bluemke, D. A.; Cooper, S. L. *Polymer* **1981**, *22*, 1428.
(67) Leung, L. M.; Koberstein, J. T. *Macromolecules* **1986**, *19*, 706.
(68) Koberstein, J. T.; Russell, T. P. *Macromolecules* **1986**, *19*, 714.
(69) Gibson, P. E.; Van Bogart, J. W. C.; Cooper, S. L. *J. Polym. Sci., Polym. Phys. Ed.* **1986**, *24*, 885.